NOVEL GEOMAGNETIC FIELD MORPHOLOGICAL CRITERIA: FROM MODERN TO PLEISTOCENE ERAS

Presented by
Dr. Filipe **TERRA-NOVA** (CNES-POSDOC)
in
ANR DYRE-COMB meeting II, Nantes 2024

Terra-Nova, F., Wardinski, I., Panovska, S., Korte, M., Novel geomagnetic field morphological criteria: from modern to Pleistocene eras. JGR: Solid Earth, (Submitted).

Nantes Université LPG cnes anr

Classical criteria of geomagnetic field morphology

Axial dipolarity
(Glatzmaier et al., 1999)

Equatorial symmetry
(Coe and Glatzmaier, 2006)

Zonality
(Christensen et al., 2010)

Flux concentration
(Christensen et al., 2010)

Four criteria **to evaluate** the **Earth likeness** of numerical dynamo simulations
(Christensen et al. 2010)

Classical criteria of geomagnetic field morphology

Axial dipolarity at the CMB
(Glatzmaier et al., 1999)

$$\mathrm{AD/NAD} = \frac{(g_1^0)^2}{(g_1^1)^2 + (h_1^1)^2 + \sum_{\ell=2}^{\ell_{max}} \left(\left(\frac{a}{c}\right)^{2\ell-2} \left(\frac{\ell+1}{2}\right) \sum_{m=0}^{\ell} (g_\ell^m)^2 + (h_\ell^m)^2 \right)}$$

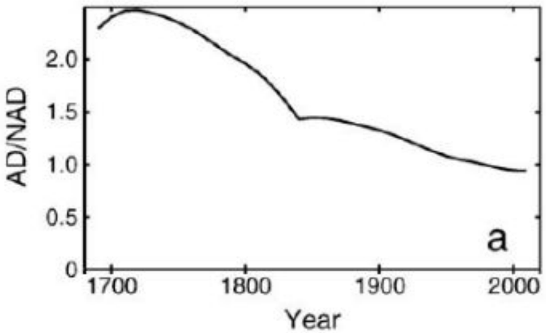

Christensen et al. (2010)

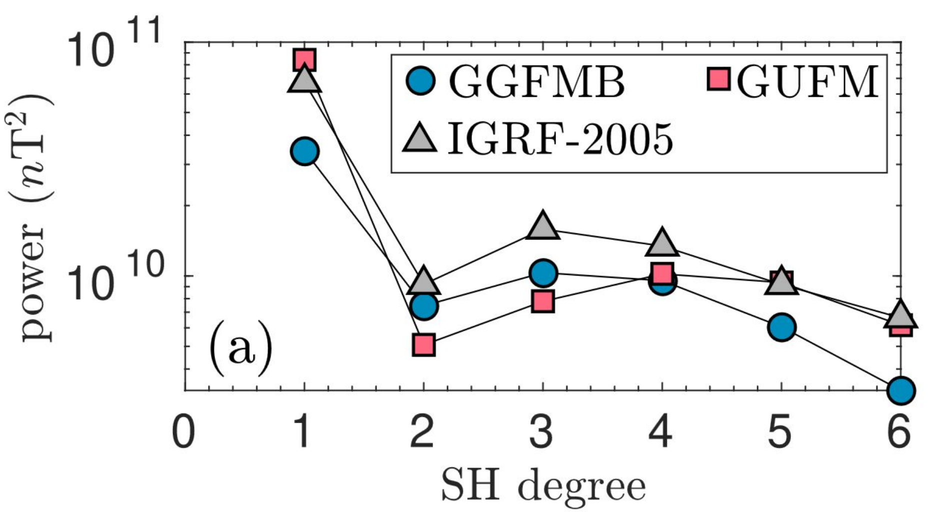

Mahgoub et al. (2023)

- **Present-day** field **dipole dominated.**
- The **lowest** values of **AD/NAD** (< 10-2) are found in periods of **transitional field** (reversals, excursion).

Classical criteria of geomagnetic field morphology

Equatorial symmetry at the CMB
(Coe and Glatzmaier, 2006)

$$\mathrm{O/E} = \frac{\sum_{\ell=2}^{\ell_{max}} \left((\ell+1) \left(\frac{a}{c}\right)^{2\ell+4} \sum_{m=0}^{\ell} \left((g_\ell^m)^2 + (h_\ell^m)^2 \right) \right) \text{ if } \ell + \mathrm{m \ odd}}{\sum_{\ell=2}^{\ell_{max}} \left((\ell+1) \left(\frac{a}{c}\right)^{2\ell+4} \sum_{m=0}^{\ell} \left((g_\ell^m)^2 + (h_\ell^m)^2 \right) \right) \text{ if } \ell + \mathrm{m \ even}}$$

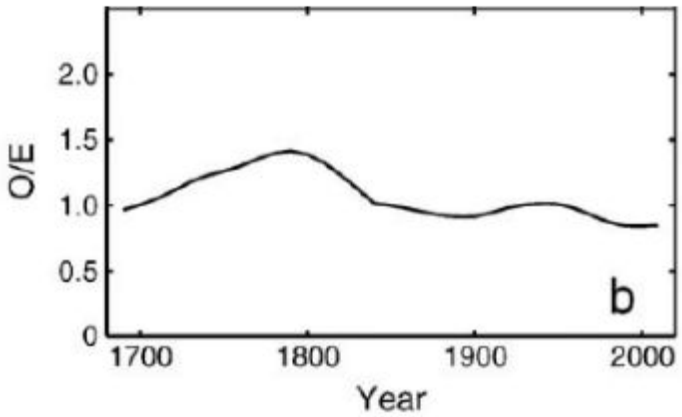

Christensen et al. (2010)

For an average of 10000 random equipartitioned magnetic field with ℓmax = 5, 8 and 13, O/E is 0.806, 0.818 and 0.841.

Larger values than equipartitioned ⟶ Equatorial Anti-symmetry

Classical criteria of geomagnetic field morphology

Zonality at the CMB
(Christensen et al., 2010)

$$Z/NZ = \frac{\sum_{\ell=2}^{\ell_{max}} \left((\ell+1) \left(\frac{a}{c}\right)^{2\ell+4} ((g_\ell^0)^2 + (h_\ell^0)^2) \right)}{\sum_{\ell=2}^{\ell_{max}} \left((\ell+1) \left(\frac{a}{c}\right)^{2\ell+4} \sum_{m=1}^{\ell} ((g_\ell^m)^2 + (h_\ell^m)^2) \right)}$$

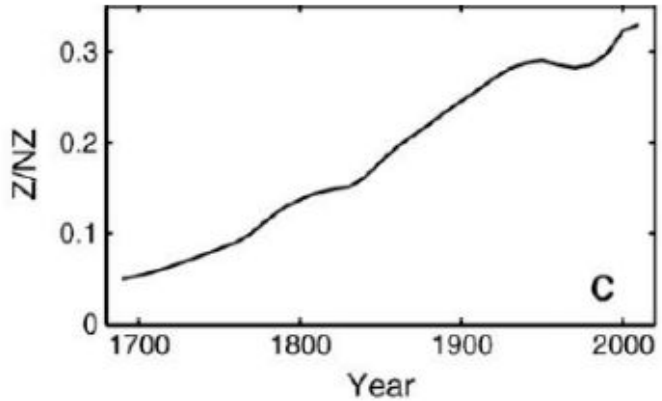

Christensen et al. (2010)

For a mean of 10000 random equipartitioned magnetic fields with ℓ_{max} = 5, 8 and 13, Z/NZ is 0.183, 0.145 and 0.112

Larger values than equipartitioned ⟶ Field organized in W-E belts

Classical criteria of geomagnetic field morphology

Flux concentration of the radial field at CMB
(Christensen et al., 2010)

$$\mathrm{FCF} = \frac{\langle B_r^4 \rangle - \langle B_r^2 \rangle^2}{\langle B_r^2 \rangle^2}$$

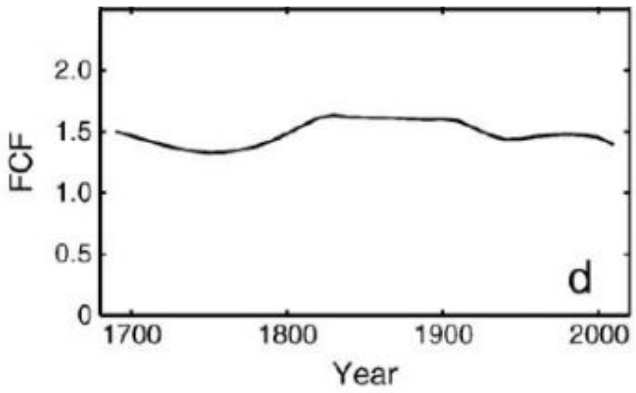

Christensen et al. (2010)

Pure dipole field: FCF = 0.8
With AD/NAD=1.4 and equipartitioned non-dipole field with ℓ_{max} = 8, FCF=1.49
(Christensen et al., 2010)

The **variance of the Br squared** evaluates the **prominence of flux patches** in the CMB.

Novel criteria of geomagnetic field morphology

Regions of weak field

Surface intensity field minimum anomaly

Polar minima magnitude

Mantle control

Flux patch duet

Polar minima dichotomy

Four **auxiliary** criteria to evaluate the Earth likeness of numerical dynamo simulations

Novel criteria of geomagnetic field morphology

Surface intensity field minimum anomaly

$$F^*_{min} = \frac{F_{min}}{\langle F \rangle}$$

For a pure axial dipole field $F^*_{min} \approx 0.725$

For a constant F, $F^*_{min} = 1.0$ (maximum value)

How **deep** is the surface **field minimum** in respect to the field everywhere else.

Novel criteria of geomagnetic field morphology

Polar minima magnitude

$$\mathrm{PM} = \begin{cases} \frac{|B_r^{NP} - min(B_r)|}{max|B_r^z|}, & \text{in the Northern Hemisphere} \\ \frac{|B_r^{SP} - max(B_r)|}{max|B_r^z|}, & \text{in the Southern Hemisphere} \end{cases} \qquad \mathrm{PMM} = \frac{\mathrm{PM_{NH}} + \mathrm{PM_{SH}}}{2}$$

Lézin et al. (2023)

For a pure dipole field with a $\theta_{dip} = 20.43^{\circ}$ (maximum tilt in the GGF100k model of Panovska et al. (2018)), PMM is ≈ 0.067

Here we consider the **existence** of **polar minima** for **PMM larger than 0.067**

How **prominent polar minima are** in respect to the maximum field value

Novel criteria of geomagnetic field morphology

Flux patch duet

1. The latitudinal average of Br squared at the CMB
2. Apply FFT: $X_j = \sum_{\kappa=0}^{N-1} A_\kappa W^{j\kappa}, j = 0, 1, ..., N-1$
3. Infer FPD from the FFT amplitude coefficients:

$$\text{FPD} = \frac{A_2}{(A_1 + A_3 + ... + A_{\ell_{max}})/(N-1)}$$

Order 2 longitudinal organization of the radial field **structures at the CMB**

Novel criteria of geomagnetic field morphology

Polar minima dichotomy

$$\mathrm{PM} = \begin{cases} \frac{|B_r^{NP} - min(B_r)|}{max|B_r^z|}, & \text{in the Northern Hemisphere} \\ \frac{|B_r^{SP} - max(B_r)|}{max|B_r^z|}, & \text{in the Southern Hemisphere} \end{cases}$$

$$\mathrm{PMD} = \mathrm{PM_{NH}} - \mathrm{PM_{SH}}$$

Lézin et al. (2023)

1. Stronger polar minima in the Northern/Southern hemisphere

↓

positive/negative PMD values

2. Small differences between Northern and Southern hemisphere

↓

PMD approaches zero

Quantification of polar minima magnitude hemisphericity

Rating of compliance

Individual score for each criteria by

$$\chi_i^2 = \left(\frac{\ln \Pi_i - \ln \Pi_i^E}{\ln \sigma_i^E}\right)^2$$

Interval for good score ($\chi_i^2 = 1.0$)

$$[\Pi_i^E / \sigma_i^E ; \Pi_i^E \sigma_i^E]$$

Christensen et al. (2010) choice of values based on a **historical field model** (Jackson et al., 2000) truncated at ℓ_{max}**=13**, **archeomagnetic field model** CALS7k.2 ℓ_{max}**=5** (Korte and Constable, 2005) and **paleomagnetic data set** (Tauxe et al., 2007):

$\sigma_{AD/NAD} = \sigma_{O/E} = 2$; $\sigma_{Z/NZ} = 1.5$; $\sigma_{FCF} = 1.5$

Scoring assignment

$$\chi^2 = \sum_i \chi_i^2$$

Quantifying Earth likeness

Level of compliance:

- ➔ $\chi^2 < 2$ *excellent*
- ➔ $2 < \chi^2 < 4$ *good*
- ➔ $4 < \chi^2 < 8$ *marginal*
- ➔ $8 < \chi^2$ *no complicance*

Spatial resolution dependence

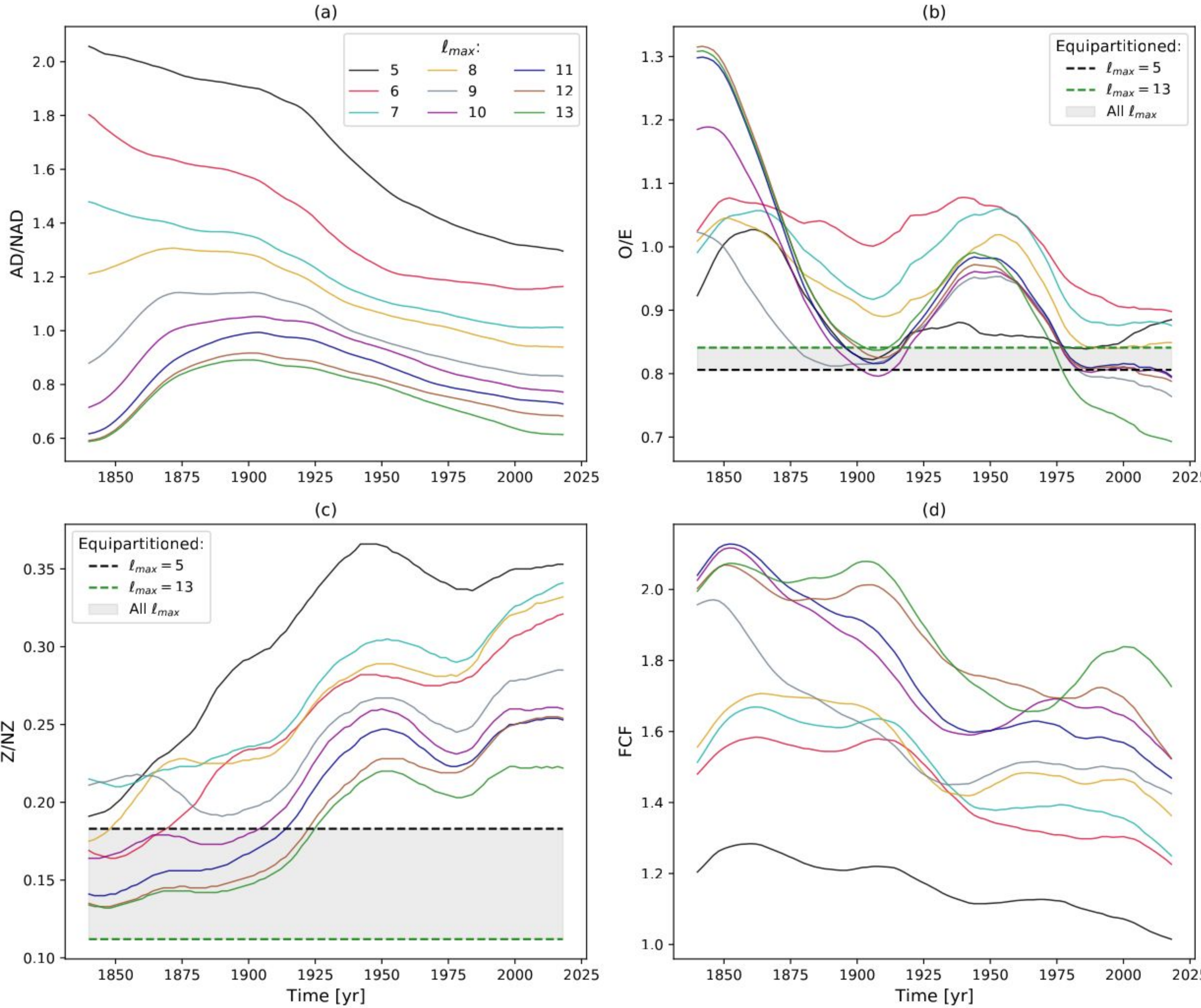

Time-averages:

- AD/NAD value is 0.45 times smaller from ℓmax = 5 to ℓ_{max} = 13
- O/E weakly dependent on ℓ_{max}
- Z/NZ decreases with increasing ℓ_{max}
- FCF increases with increasing ℓ_{max}

Spatial resolution dependence

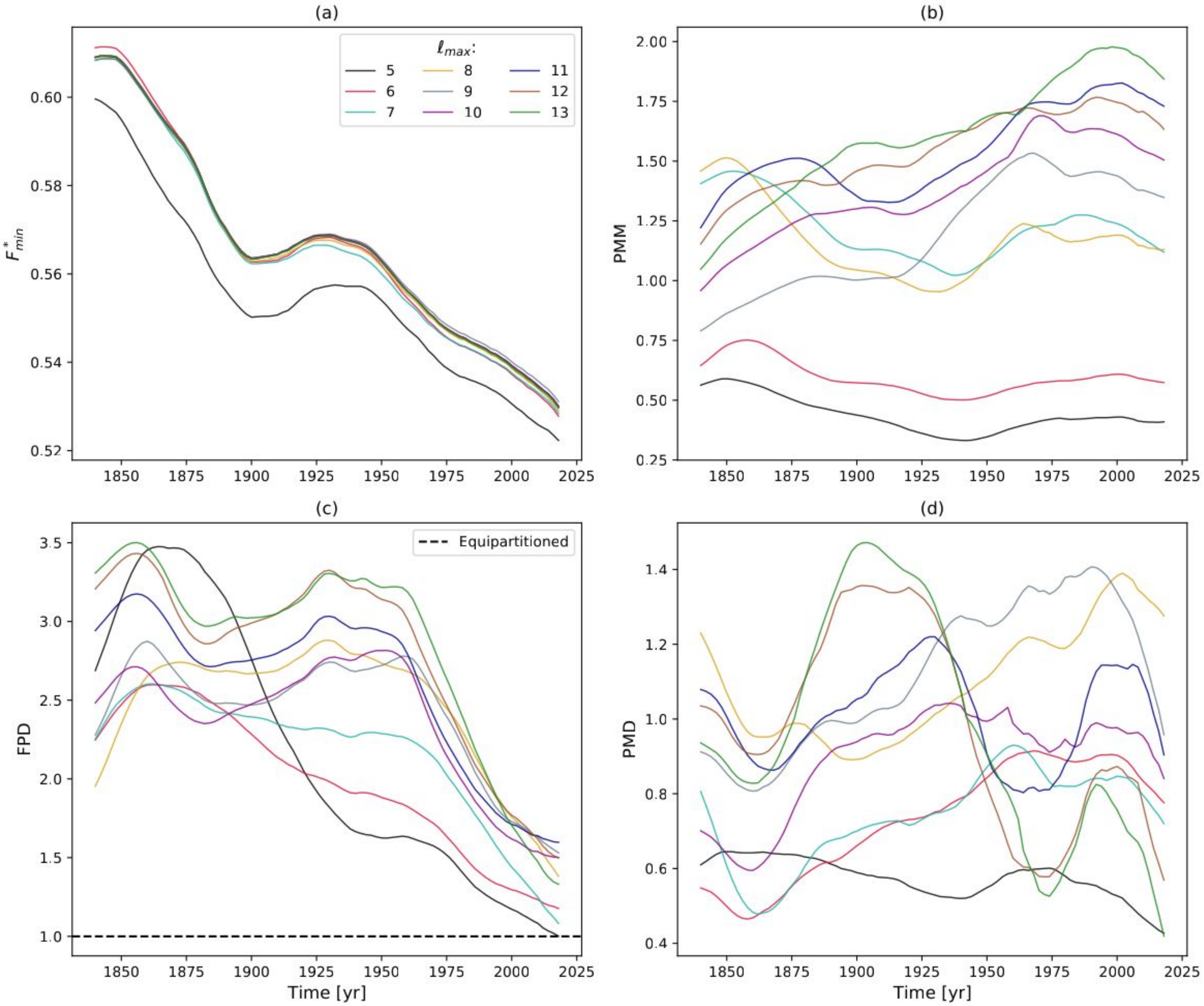

Time-averages:

- F^*_{min} is weakly dependent on ℓ_{max}
- PMM increases drastically with increasing ℓ_{max}
- FPD increases (though not monotonically) with ℓ_{max}

Suite of geomagnetic field models

Model name	Reference	ℓ_{max}	Data type	Modeling	Period	Time interval	Δt
CHAOS7.13	Finlay et al. (2020)	14	St & O	SI	Modern	1997 AD - 2022 AD	1
KALMAG	Baerenzung et al. (2022)	14	St & O & H	BI	Historical	1900 AD - 2016 AD	8
GUFM1	Jackson et al. (2000)	14	O & H	SI	Historical	1840 AD - 1990 AD	2.5
COV-OBS.x2	Huder et al. (2020)	14	St & O & H	BI	Historical	1840 AD - 2018 AD	2
BIGMUDIh.1	Arneitz et al. (2021)	14	O & H & A & L	BI	Historical	1380 AD - 1920 AD	3.5
HistKalmag	Schanner et al. (2023)	14	O & H & A & L	BI	Historical	1000 AD - 1940 AD	10
SHAWQ2k	Campuzano et al. (2019)	10	A & L	SI	Archeological	0000 AD - 1900 AD	20
ARCH3k	Korte et al. (2009)	14	A & L	SI	Archeological	1000 BC - 1900 AD	5
A_FM-M	Licht et al. (2013)	5	A & L	SI	Archeological	1000 BC - 1900 AD	40
ASD_FM-M	Licht et al. (2013)	5	A & L & S	SI	Archeological	1000 BC - 1900 AD	40
ASDI_FM-M	Licht et al. (2013)	5	A & L & S	SI	Archeological	1000 BC - 1900 AD	40
COV-ARCH	Hellio and Gillet (2018)	10	A & L	BI	Archeological	1000 BC - 1900 AD	100
COV-LAKE	Hellio and Gillet (2018)	10	A & L & S	BI	Archeological	1000 BC - 1900 AD	100
BIGMUDI4k	Arneitz et al. (2019)	8	H & A & L	BI	Archeological	1000 BC - 1900 AD	20
SHA.DIF.14k	Pavón-Carrasco et al. (2014)	10	A & L	BI	Holocene	5000 BC - 1850 AD	50
ArchKalmag14k	Schanner et al. (2022)	14	A & L	BI	Holocene	6000 BC - 1900 AD	50
pfm9k.2	Nilsson et al. (2022)	8	A & L & S	BI	Holocene	7000 BC - 1900 AD	10
HFM.OL1.A1	Constable et al. (2016)	10	A & L & S	SI	Holocene	8000 BC - 1900 AD	10
CALS10K.2	Constable et al. (2016)	10	A & L & S	SI	Holocene	8000 BC - 1900 AD	10
LSMOD.2	Korte et al. (2019)	10	A & L & S	SI	Pleistocene	48k BC - 28k BC	50
GGFSS70	Panovska et al. (2021)	6	S	SI	Pleistocene	70k BC - 14k BC	100
GGF100k	Panovska et al. (2018)	10	A & L & S	SI	Pleistocene	100k BC - 1650 BC	200
GGFMB	Mahgoub et al. (2023)	6	S	SI	Pleistocene	900K BC - 700k BC	200

23 geomagnetic field models grouped by 'era':
1 Modern, **5** historical, **8** Archeological, **5** Holocene and **4** Pleistocene

Axial dipolarity

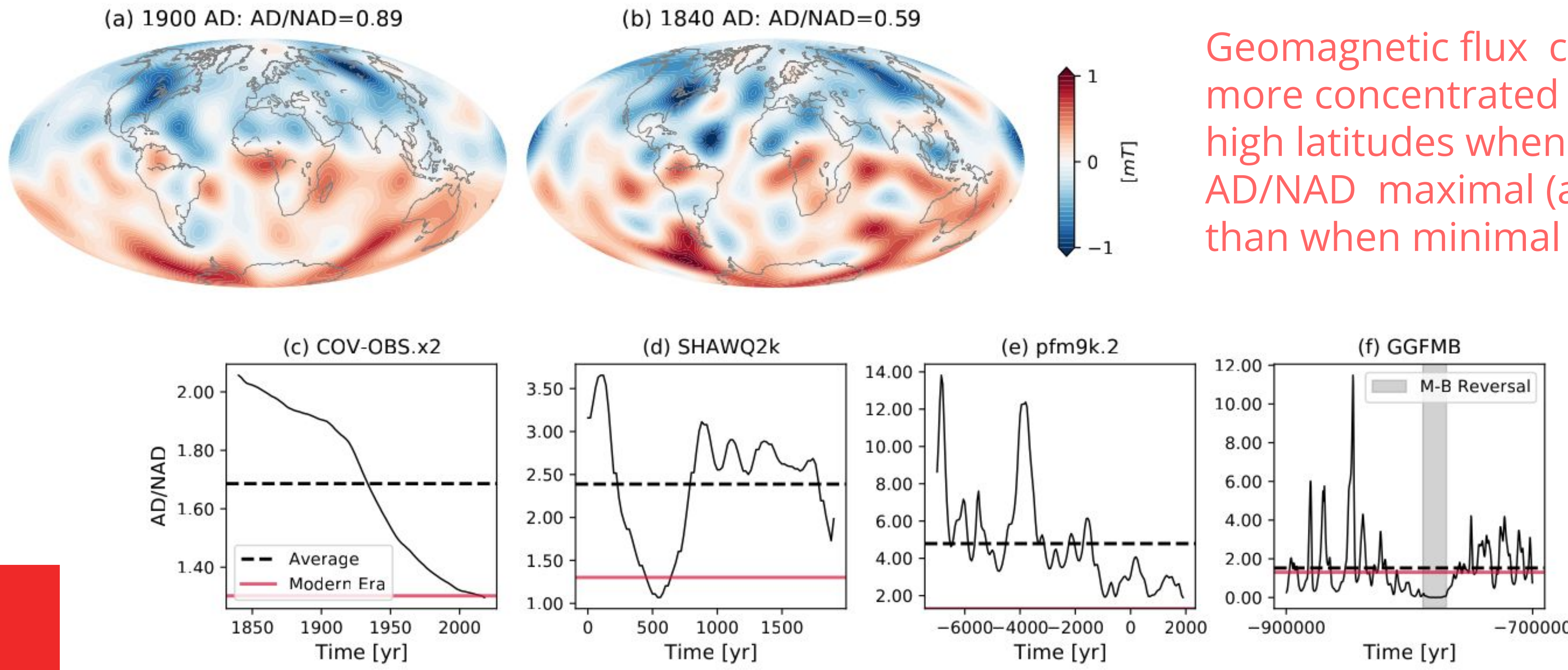

Geomagnetic flux clearly more concentrated at high latitudes when AD/NAD maximal (a) than when minimal (b).

- From 1840 AD to 2019 AD, AD/NAD decreased from 2.05 to 1.30
- SHAWQ2k briefly dipped below the modern value around 600 AD
- pfm9k.2 always above present-day values
- Obviously GGFMB had much lower AD/NAD values during the latest reversal as well as at other times.

Equatorial symmetry

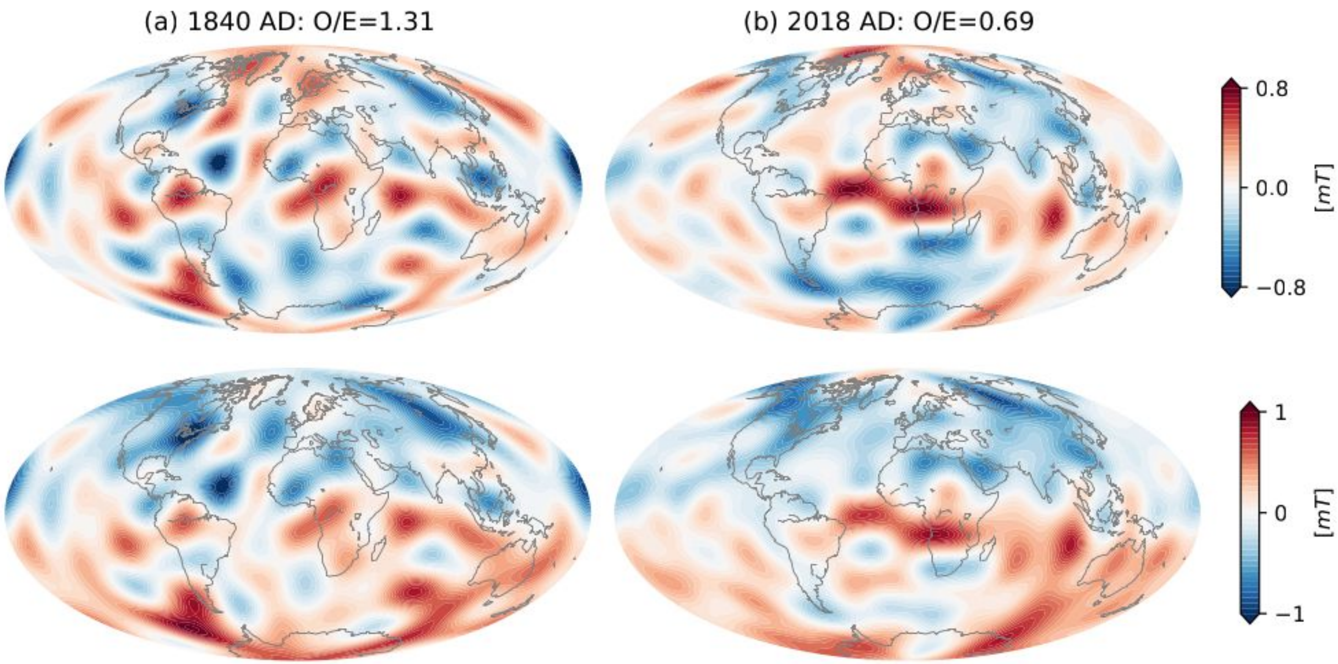

(a) Intense flux patches in the NH and SH correlate in longitude leading to a considerable O/E value of 1.35.

(b) Reversed flux region, below the South Atlantic stretched to the West leading to a significant reduction of the O/E ratio

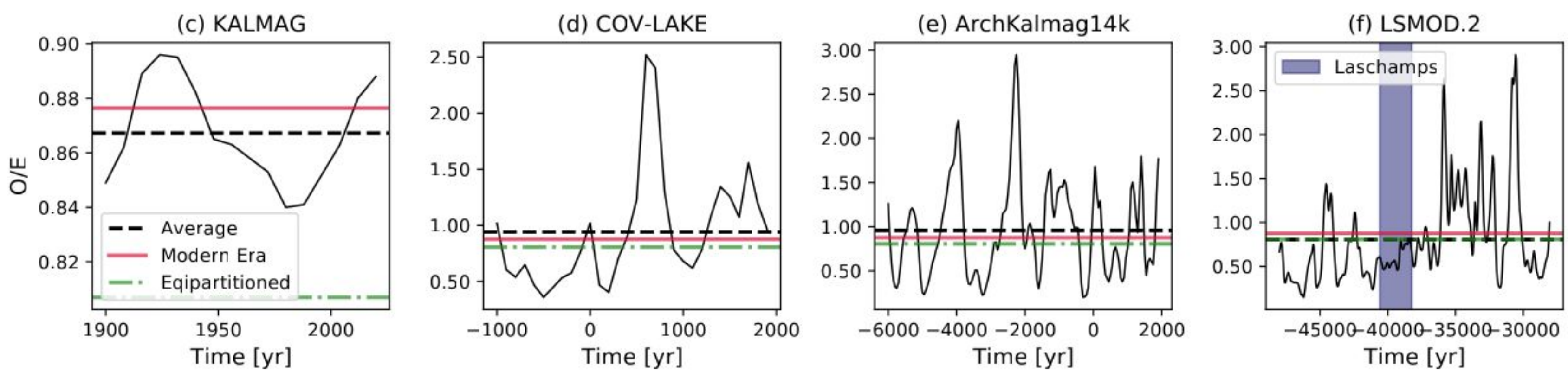

- **Historical** field **less anti-symmetric** than the **modern** on average
- Archeo and Holocene O/E values are highly time dependent and their time-averages are larger
- **Symmetry** dominated the **field** during the Laschamps **excursion**

Zonality

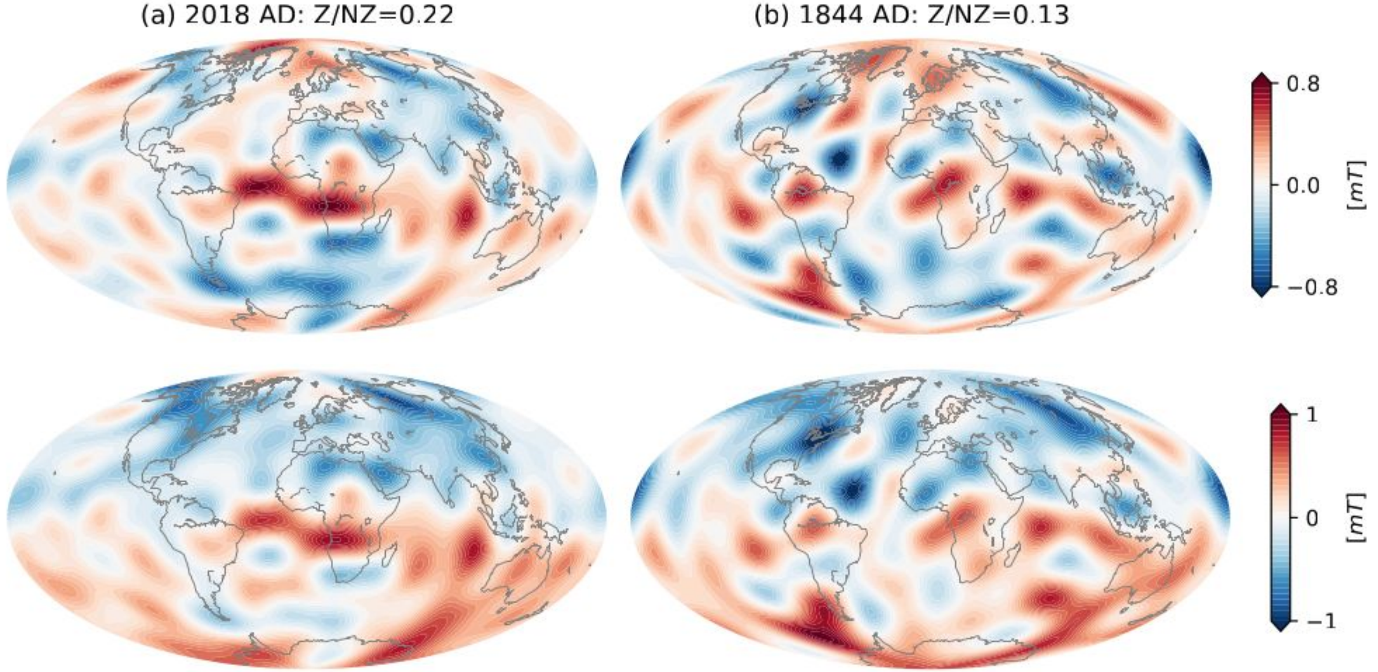

(a) two W-E belts at the equator and below the South Atlantic lead to large Z/NZ.

(b) much less prominent W-E belts.

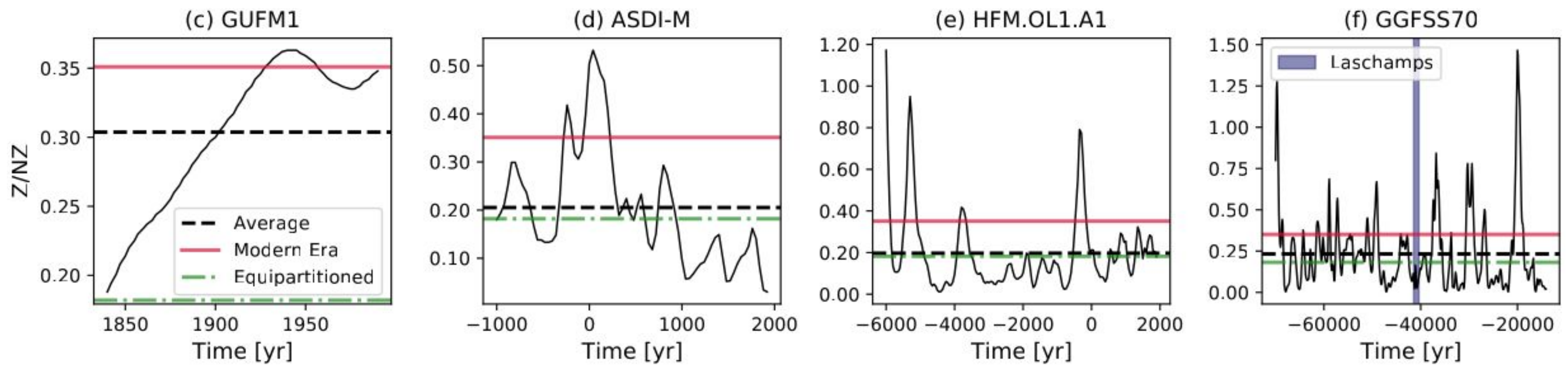

- **Historical** field has become **more zonal** until a maximum around 1940.
- **Archeological** field model is **much less zonal**.
- Holocene presents episodes of both much stronger non-zonalily/zonalily.
- Laschamps **excursion** characterized by **weak zonality**.

Flux concentration factor

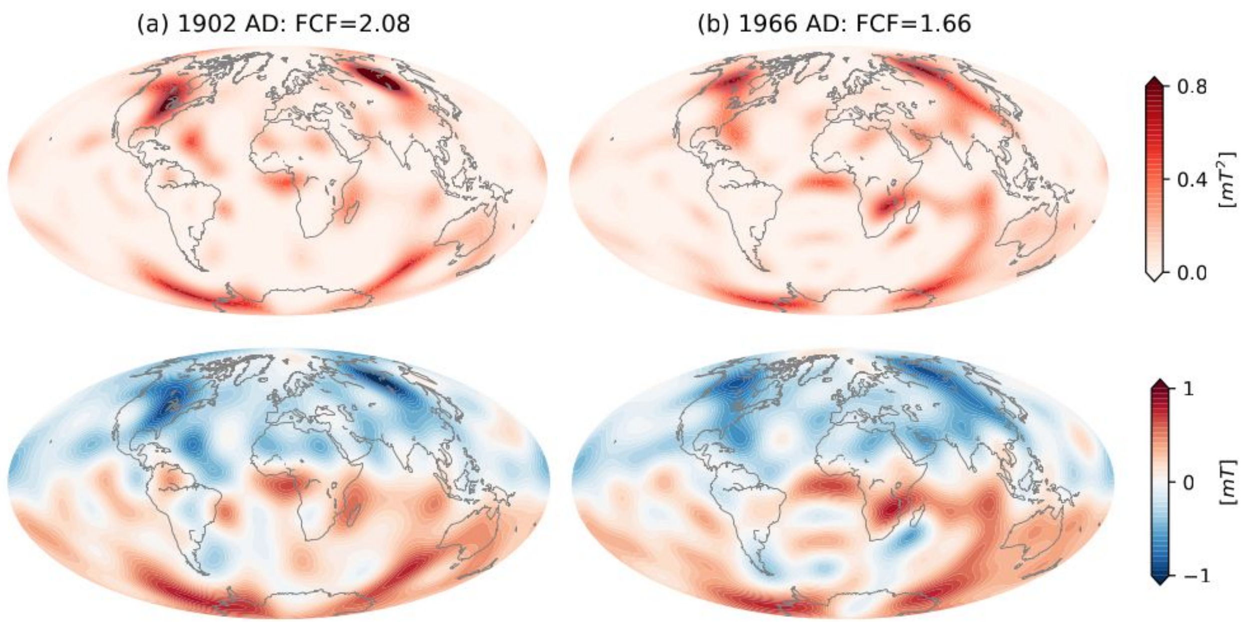

(a) **Strongly concentrated** in two pairs of intense high-latitude flux patches.

(b) Patches significantly **weaker** and in the eastern hemisphere extended over **larger areas**, hence the **FCF** value is **smaller**.

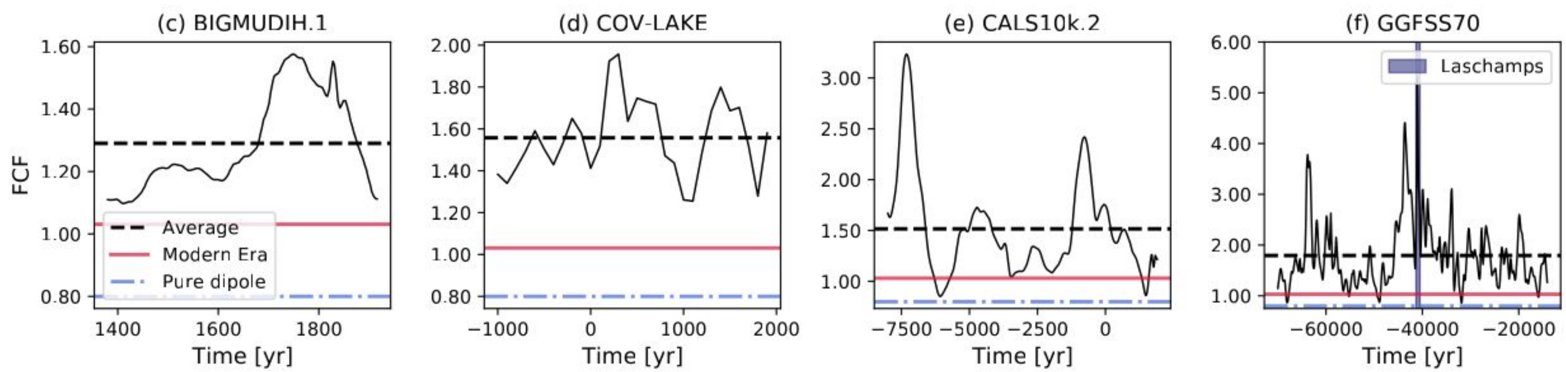

- **Seldom FCF** values of a **pure dipole field**.
- Historical and archeological field models have at all times FCF values larger than the modern field.
- **Holocene and Pleistocene** models show peaks that are up to a**bout two three times larger** than the **historical maximum FCF value**.
- The Pleistocene model exhibits an FCF peak during the Laschamps excursion.

Surface intensity field minimum anomaly

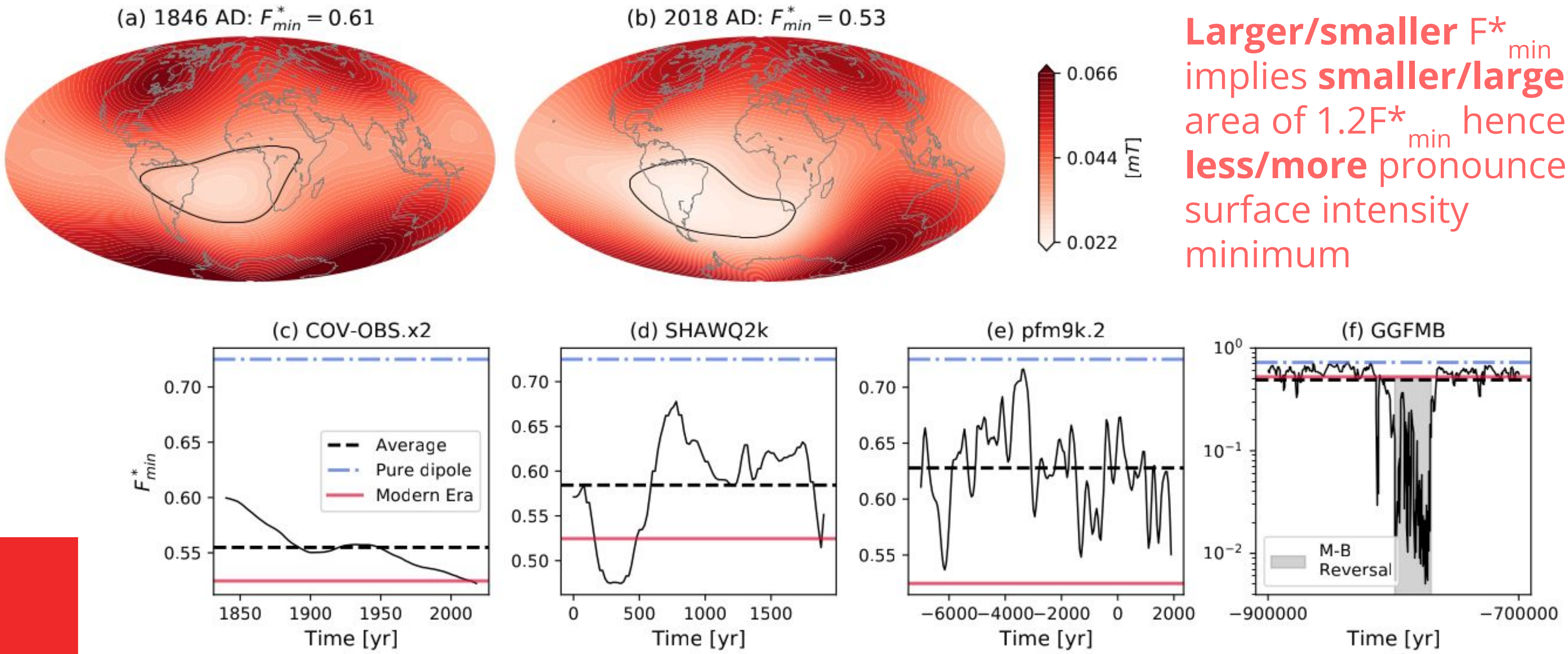

Larger/smaller F^*_{min} implies **smaller/larger** area of $1.2F^*_{min}$ hence **less/more** pronounced surface intensity minimum

- Minimum getting **more prominent throughout** the **historical** period.
- An episode of a significant minimum between 250–450 AD.
- In the **Holocene** model, F^*_{min} is usually **much larger than the modern value**.
- **Extremely low values** of F^*_{min} in Pleistocene models, O(−2), **during excursions or reversals**.

Polar minima magnitude

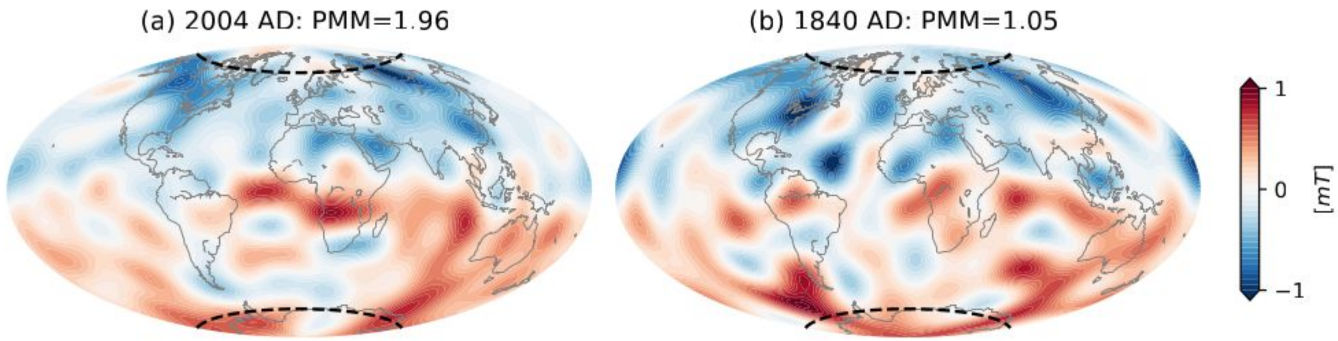

- **Largest PMM** value has **reversed flux patches** at both geographical poles
- **Normal flux** covers the poles when the **smallest PMM** is found

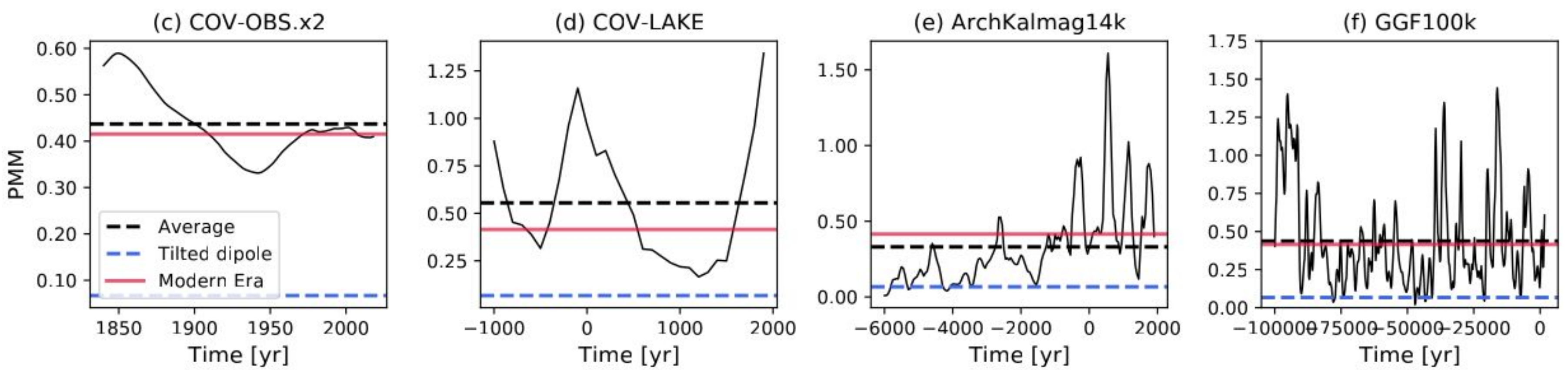

- **Historical field** shows a **decrease in the PMM** value until 1940 AD
- **Although** some models have **close PMM values to the present-day field**, they show **much stronger time dependence**

Flux patch duet

- **Two** antipodal peaks to **one** peak **from 1860 to 2018 AD** where the peak at ≈ 90° W vanished
- FPD time dependence reflects differences in **morphology** in the **Southern hemisphere**

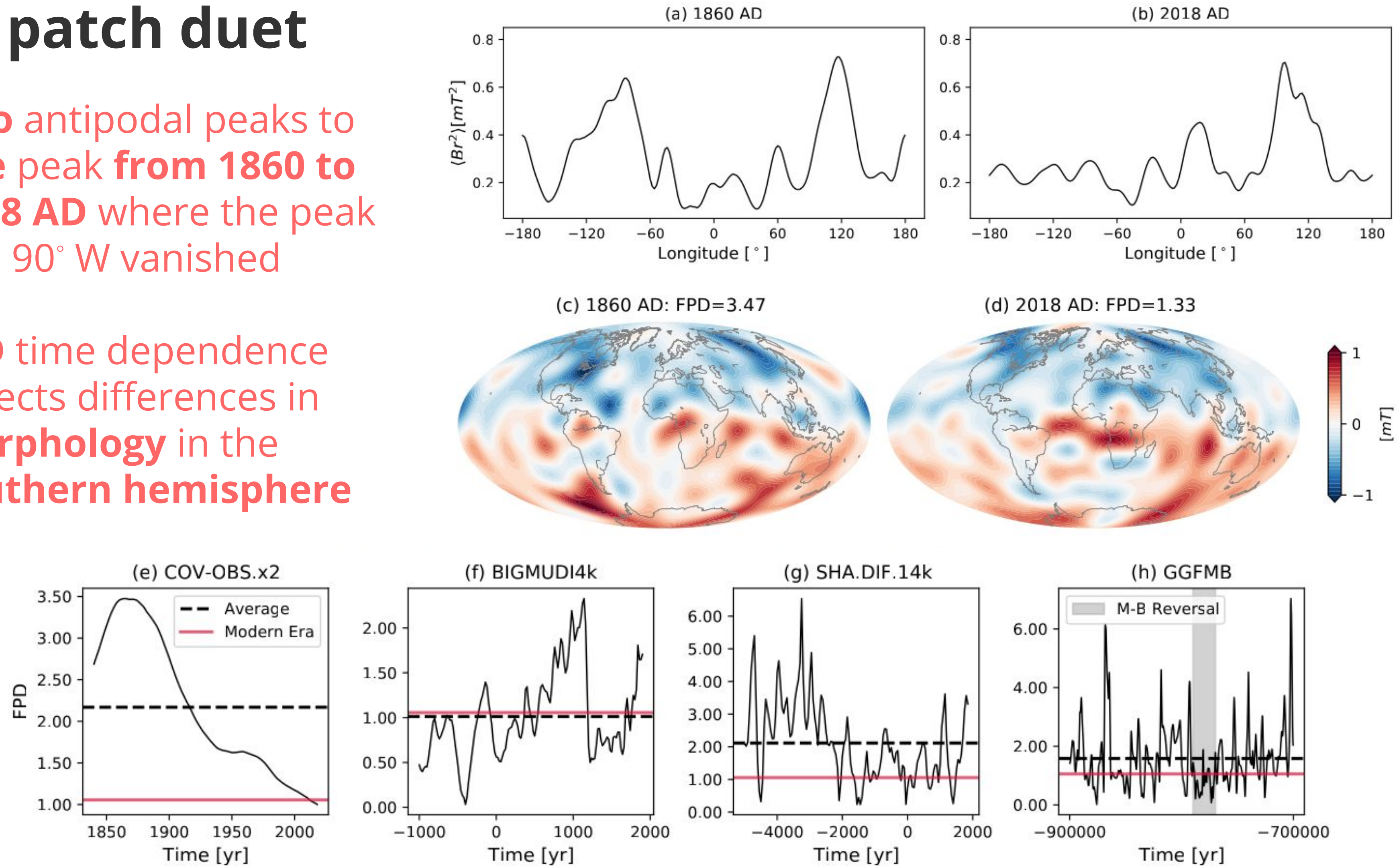

- **FPD** ratio has **continuously decreased** from 1860 AD **until present.**
- **Ancient** models have **intermittent large/small FPD**
- Holocene has long episodes of high FPD value between ≈ 6000 BC and 2200 BC
- The FPD in the Pleistocene reaches values larger than 6.00

Polar minima dichotomy

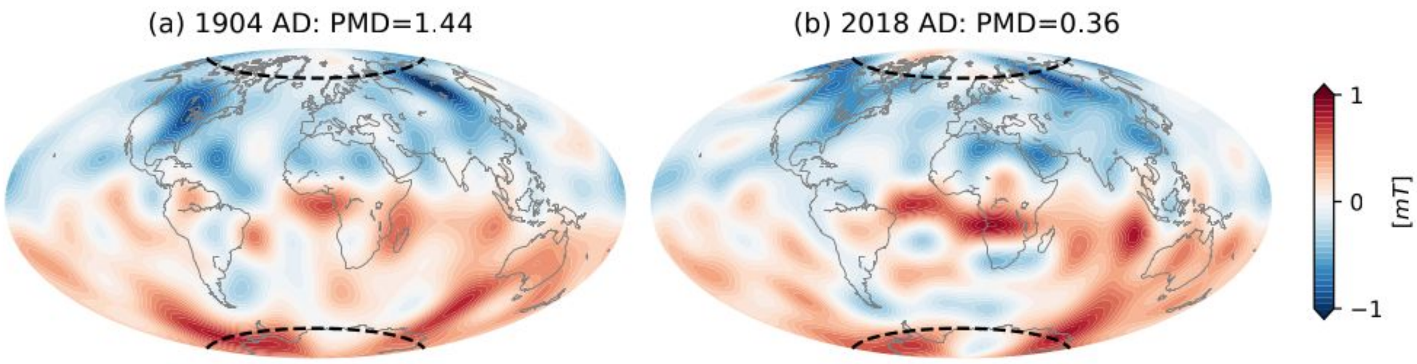

(a) inside the Northern TC a reversed flux patch prevails while inside the Southern TC the polarity is normal

(b) reversed flux patches prevail inside the TC at both hemispheres

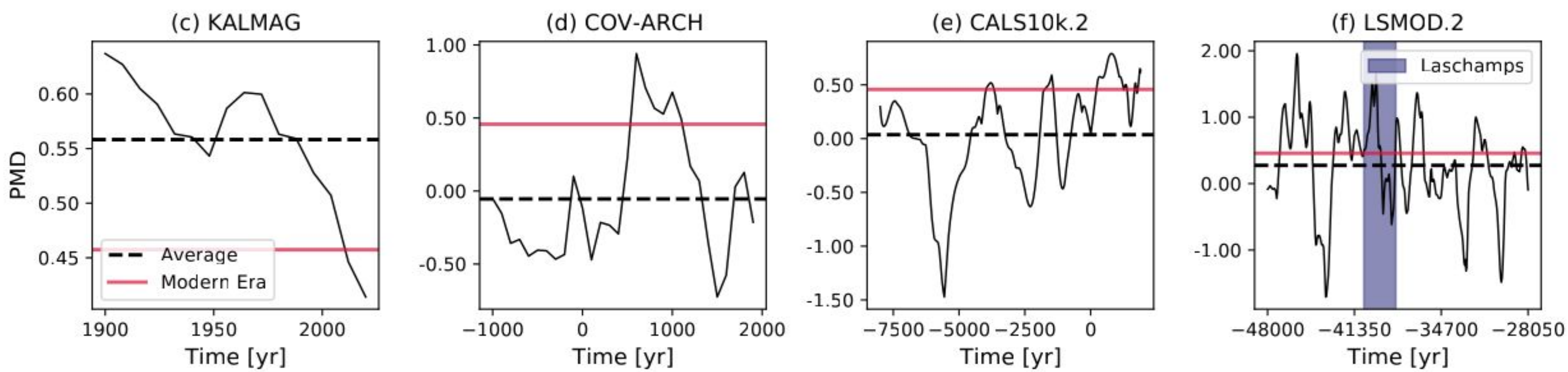

- The value of PMD in general decreases during the historical era, but still maintains a significant positive value until present
- The ancient models show episodes of stronger northern and at times stronger southern polar minima, some periods larger PMD values than modern era
- Extreme PMD values found during transitional fields but not exclusive to those

New bounds for Earth likeness

Christensen et al. (2010) choice of values based on a **historical field model** (Jackson et al., 2000) truncated at ℓ_{max}**=13**, **archeomagnetic field model** CALS7k.2 ℓ_{max}**=5** (Korte and Constable, 2005) and **paleomagnetic data set** (Tauxe et al., 2007)

- **New bounds** based on the **mean** values of **all models of a specific era**
- σ_{F^*min} attributes $\chi^2_{F^*min}$ ≈ 1.36 to **a pure dipole field**
- Since all periods have **positive PMD**, σ_{PMD} attributes χ^2_{PMD} ≈ 1.10 to a field with PMD equals to zero

	AD/NAD	O/E	Z/NZ	FCF	F^*_{min}	PMM	FPD	PMD
From Christensen et al. (2010)								
Π_i^E	1.40	1.00	0.15	1.50	-	-	-	-
Modern era truncated at $\ell_{max} = 8$								
Π_i^E	0.94	0.84	0.33	1.40	0.49	1.15	1.53	1.31
Modern era truncated at $\ell_{max} = 5$								
Π_i^E	1.30	0.88	0.35	1.03	0.52	0.42	1.06	0.46
Historical era								
Π_i^E	1.88	0.87	0.30	1.19	0.56	0.43	1.72	0.46
Archeological era								
Π_i^E	2.83	0.87	0.24	1.26	0.59	0.39	1.50	0.06
Holocene era								
Π_i^E	4.01	1.03	0.23	1.38	0.62	0.40	1.78	0.16
Pleistocene era								
Π_i^E	1.80	0.91	0.28	1.93	0.49	0.59	1.60	0.12
All eras								
σ_i^E	2.00[a]	2.00[a]	2.50[a]	1.75[a]	1.40	2.00	2.00	1.55

[a] from Christensen et al. (2010). Π_i^E is the target value and σ_i^E represents how much the value can depart from its mean to score well.

Rating of compliance with present-day field

To quantify the semblance of past fields to the present-day field

Weak compliance of several models of the ancient field built with distinctive periods, data sets and modeling methodologies may suggest a **highly time-dependent geodynamo**

Alternatively, it may indicate that the models morphological criteria are **limited by their data sets and methodologies**

Model	$\langle\chi^2\rangle$	$\min(\chi^2)$	τ_χ^2	$\langle\chi'^2\rangle$	$\min(\chi'^2)$	$\tau_{\chi'^2}$
Historical						
KALMAG	0.06	0.00	100/0/0/0	0.54	0.00	100/0/0/0
GUFM1	0.30	0.01	100/0/0/0	1.27	0.07	84/16/0/0
COV-OBS.x2	0.21	0.00	100/0/0/0	0.98	0.00	88/12/0/0
BIGMUDIH.1	1.75	0.29	73/27/0/0	2.83	1.24	81/16/3/0
HistKalmag	1.75	0.12	56/33/6/5	4.29	0.70	45/45/6/3
Archeological						
SHAWQ2k	2.32	0.47	41/32/21/6	7.20	1.24	31/31/27/10
ARCH3k	3.42	0.47	15/49/27/10	6.79	2.15	23/38/23/17
A_FM	4.30	1.25	4/45/38/14	6.71	2.37	8/51/19/22
ASD_FM	3.48	0.26	24/43/28/4	6.70	2.72	16/47/30/7
ASDI_FM	3.99	0.67	18/32/45/5	6.86	4.37	0/61/32/7
COV-ARCH	1.19	0.45	77/17/7/0	4.91	1.28	37/47/17/0
COV-LAKE	3.17	0.65	33/33/33/0	7.55	1.35	17/37/37/10
BIGMUDI4k	1.57	0.43	66/16/18/0	2.76	0.68	72/12/12/5
Holocene						
SHA.DIF.14k	4.80	0.97	12/28/37/23	8.31	1.88	13/36/28/24
ArchKalMag14k	4.23	0.21	18/28/35/20	8.63	0.52	14/27/28/31
pfm9k.2	4.83	0.43	12/22/42/23	8.72	1.86	12/33/29/26
HFM.OL1.A1	5.00	0.42	13/23/49/15	11.19	2.15	1/22/33/43
CALS10K.2	4.28	0.47	15/29/41/15	7.64	1.11	14/40/26/20
Pleistocene						
LSMOD.2	3.96	0.57	15/36/28/21	8.05	1.54	8/42/22/28
GGFSS70	4.90	0.52	14/24/38/24	12.83	0.92	4/20/23/53
GGF100k	3.33	0.32	24/37/33/6	7.43	1.42	15/41/26/18
GGFMB	5.52	0.28	12/24/30/34	11.54	2.03	6/22/25/47

$\langle\chi^2\rangle$ is the time averaged rating of compliance, $\min(\chi^2)$ the minimum χ^2 found for a snapshot and τ_χ^2 the percentage (in integer) of snapshots of a model that are excellent/good/marginal/non-compliant with respect to the modern field when considering the classical criteria (Christensen et al., 2010). $'$ indicates that both classical and novel criteria are considered.

Rating of compliance with present-day field

(a) Good old and novel

(b) Good old and bad novel (FPD too small)

(c) Bad old (AD/NAD too large) and good novel

(d) Bad old (Z/NZ too small) and novel (FPD too large)

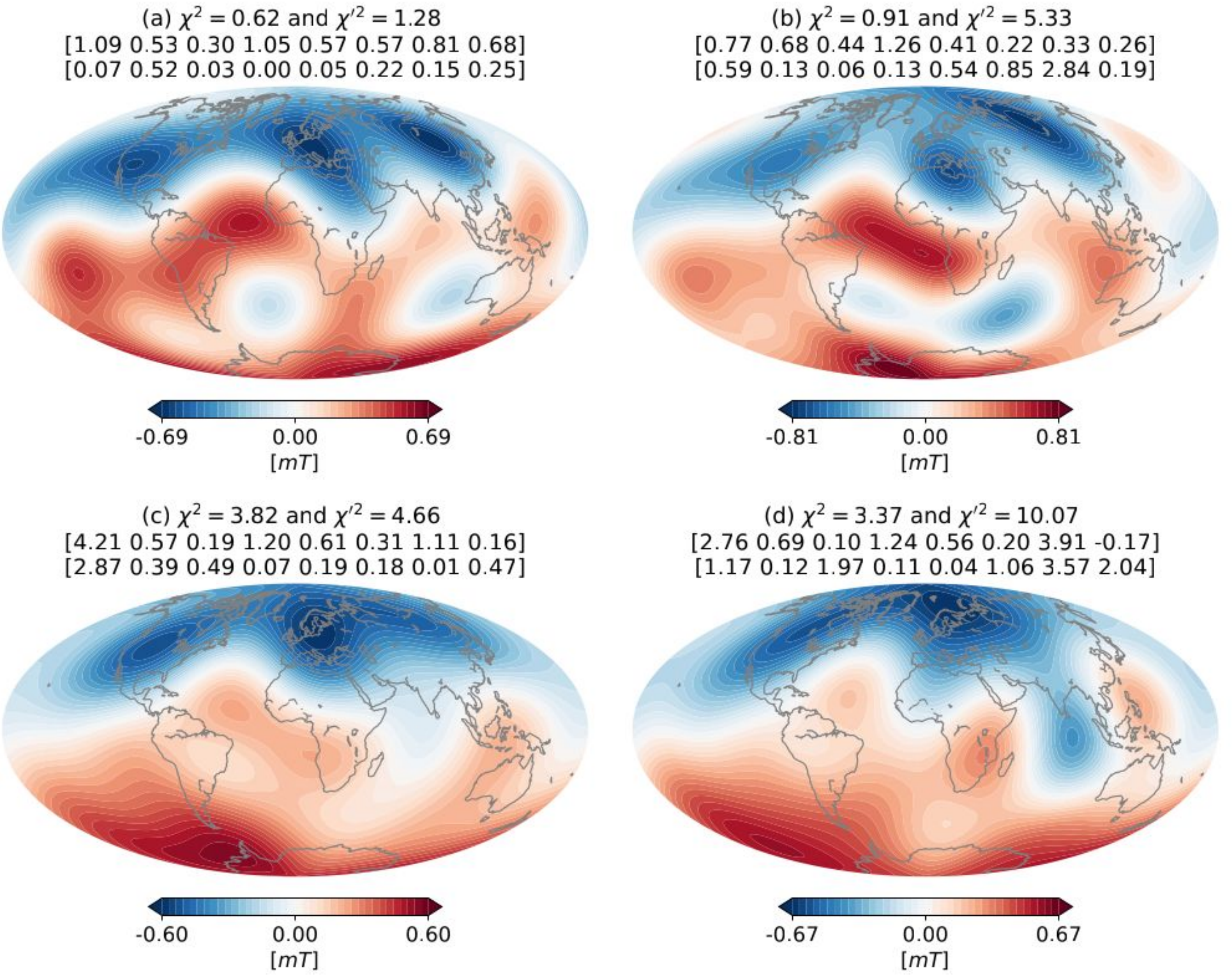

Transitional field

- An excursion if $\theta_{dip} > 45^\circ$ (Wicht, 2005)
- Duration of a transitional field is determined by $\max(\theta_{dip}) = 20.43^\circ$
- The duration of the Laschamps excursion is ≈ 2400 yr and ≈ 925 yr in LSMOD.2 and GGFSS70, respectively
- $\max(\theta_{dip})=76.30^\circ$ in LSMOD.2 and 142.20° in GGFSS70
- The duration of the Matuyama-Brunhes reversal in GGFMB is ≈ 18 kyr

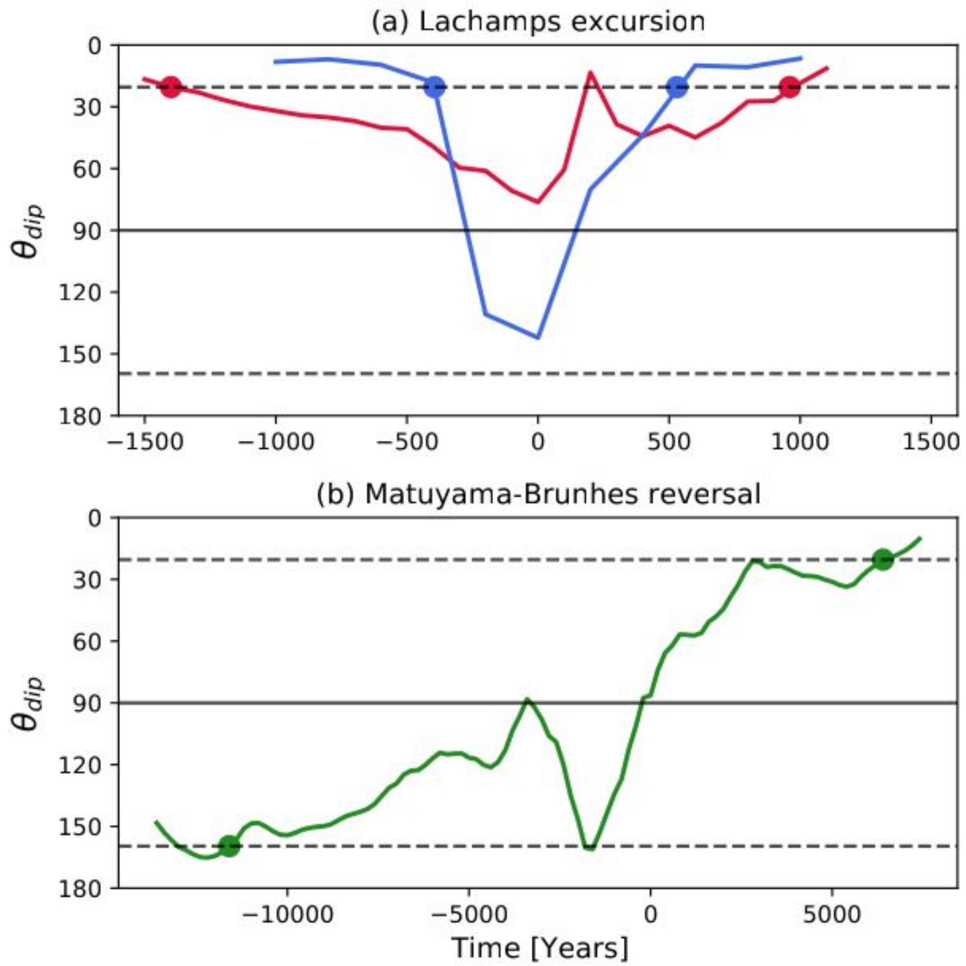

Model	AD/NAD	O/E	Z/NZ	FCF	F^*_{min}	PMM	FPD	PMD
				Laschamps excursion				
LSMOD.2	0.043(0.052)	0.63(0.12)	0.10(0.04)	1.78(0.34)	0.18(0.15)	1.96(0.30)	1.62(0.83)	0.39(0.70)
GGFSS70	0.004(0.004)	0.55(0.09)	0.06(0.04)	3.56(0.81)	0.02(0.02)	1.45(0.09)	1.12(0.19)	-0.32(0.60)
				Matuyama-Brunhes reversal				
GGFMB	0.028(0.034)	0.73(0.18)	0.20(0.14)	2.14(0.48)	0.06(0.07)	1.65(0.91)	0.73(0.38)	0.48(0.85)

Conclusions

5/8 criteria have significantly larger variations from ℓ_{max} = 5 (ancient relevant truncation) to ℓ_{max} = 6 compared to differences between other pairs of successive ℓ_{max} values

Throughout its history the geomagnetic field exhibited intermittent levels of equatorial anti-symmetry and zonality, which may be related to the transient amount of CMB reversed flux

Surface intensity minima can be used as indicators of transitional field

Large magnitudes of polar minima are consistent with weak or no stratification at the top of Earth's core

Very large values of polar minima during transitional fields suggest that reversals are triggered inside the TC

Long-term mantle control on the geodynamo is evident in the recurrent longitudinal pattern of the CMB radial field as well as in the recurrence of stronger northern than southern polar minimum

Thank you for the attention

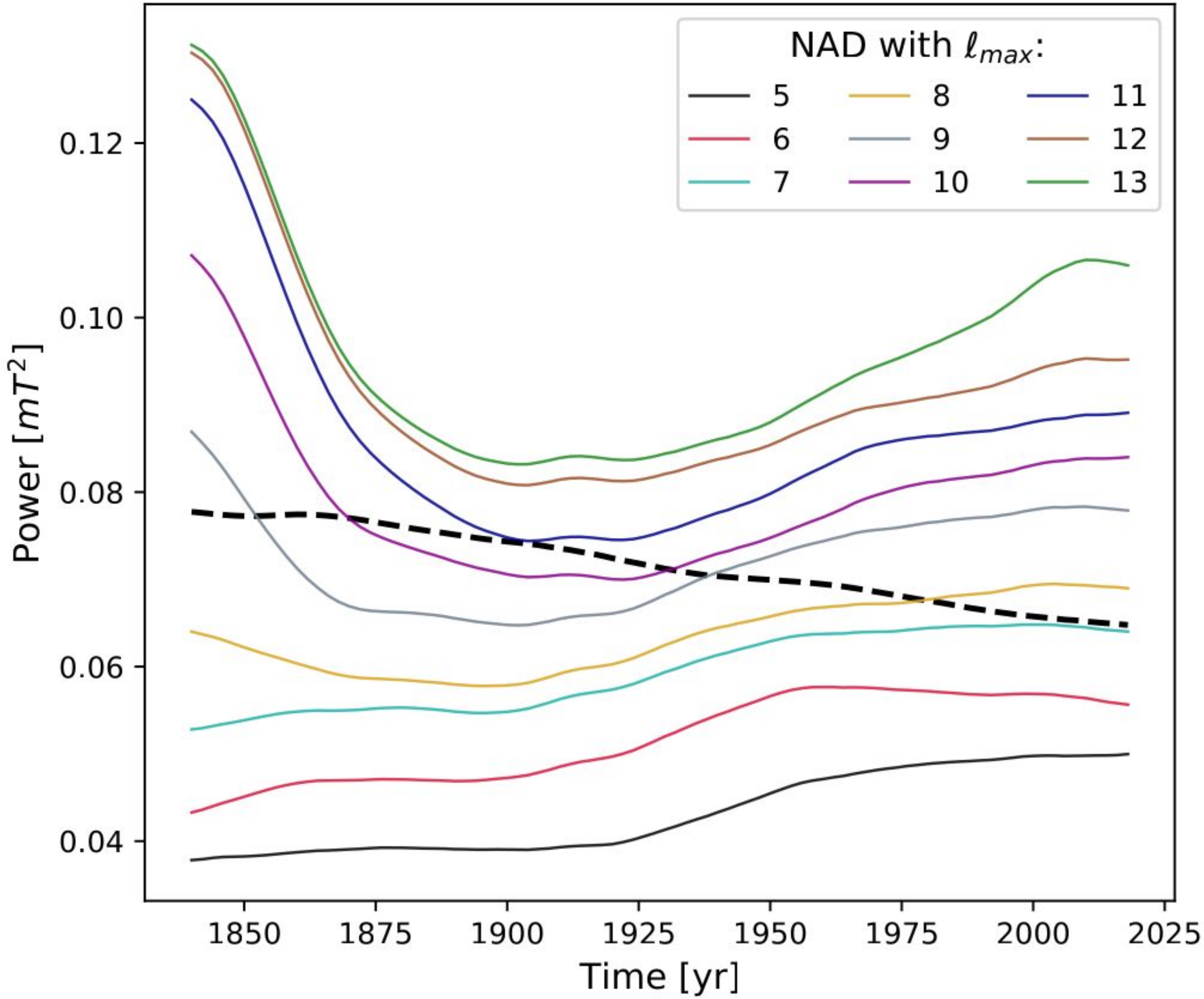

NAD with ℓ_{max}:
5
6
7
8
9
10
11
12
13
Power [mT^2]
0.04
0.06
0.08
0.10
0.12
1850
1875
1900
1925
1950
1975
2000
2025
Time [yr]